


ORIGINAL ARTICLE

Open Access



Movement Modeling and Control for Robotic Bonnet Polishing

Xuepeng Huang^{1,2}, Zhenzhong Wang^{1,2*}  and Zewen Lin^{1,2}

Abstract

With the increasing demand for high-precision optical components, bonnet polishing technology is increasingly being used in the polishing process of optical components owing to its high removal efficiency and high surface accuracy. However, it is expensive and difficult to implement dedicated bonnet polishing machine tools, and their processing range is limited. This research combines bonnet polishing technology with industrial robot-assisted processing technology to propose a robotic bonnet polishing control model for large-diameter axisymmetric aspherical optical components. Using the transformation relations of the spatial coordinate system, the transformation relations of the workpiece coordinate system, local coordinate system of the polishing point, and tool coordinate system of the bonnet sphere center are established to obtain the bonnet precession polishing motion model. The polishing trajectory of large-diameter axisymmetric aspherical components and the variation in the linkage angle difference were simulated by adding an efficiency-optimal control strategy to the motion model. The robot motion was simulated in Robostudio to verify the correctness of the precession motion model and control algorithm. Lastly, the robotic bonnet polishing system was successfully applied to the polishing process of the optical components.

Keywords: Industrial robot, Bonnet polishing, Precession movement, Control algorithm

1 Introduction

The Bonnet polishing technology was co-proposed by ZEEKO (UK) and the University of London and has been successfully applied to the polishing of optical components [1–3]. Bonnet polishing technology has a high polishing efficiency and high processing accuracy, which is a significant advantage in the processing of free-form workpieces. Among them, Walker et al. [4, 5] based on power spectral density analysis and filtering theory, solved the medium-frequency errors generated during the machining process and handled grinding errors at spatial wavelengths from 1 to 50 mm, which could be applied to manufacturing the primary mirror of the European Extremely Large Telescope (E-ELT), developed by the European Southern Observatory. Beaucamp et al. [6]

used jet and bonnet polishing techniques to machine a chemically nickel-plated aspherical mandrel workpiece with a surface roughness of just 0.6–0.8 nm, which satisfies the requirements of industrial machining and related applications, such as the manufacture of the main mirror of Japan's next-generation space telescope.

Yao et al. improved the bonnet structure [7], successfully developed a 6-axis bonnet polishing machine, conducted polishing experiments on BK7 glass material to obtain a smooth surface [8], and studied the nature of the bonnet polishing contact area [9], modeling of the precession motion [10], post-processing algorithm [11], and other related aspects. Based on the principle device and five-axis CNC bonnet polishing machine, Wang et al. [12–15] achieved optimal efficiency of bonnet polishing for aspheric and free-form surfaces by modeling and controlling algorithms of the precession motion, optimization of process parameters, and analyzing machining characteristics.

*Correspondence: wangzhenzhong@xmu.edu.cn

¹ Department of Mechanical and Electrical Engineering, Xiamen University, Xiamen 361005, China

Full list of author information is available at the end of the article

In addition to the above-mentioned research on the development of bonnet polishing machines, studies have also been conducted on the removal mechanism of bonnet polishing. Shi et al. [16, 17] revealed the material removal mechanism of the bonnet polishing process at a microscopic scale based on microscopic contact theory and friction theory and established a material removal model of abrasive grains and micro-convex bodies on the surface of polishing pads on workpieces. Cao et al. [18, 19] experimentally determined the removal mechanism of bonnet polishing on workpieces, and the results revealed that the abrasive grains in the polishing solution dominated workpiece removal. The dwell time and material removal rate were linearly related, and a multiscale predictive model of the material removal characteristics of bonnet polishing was developed.

After nearly two decades of development, bonnet polishing technology has been mostly perfected. However, because the bonnet polishing machine tool is expensive and occupies a large space, and the general size of the bonnet polishing machine makes it difficult to process large-diameter components, limiting the promotion of bonnet polishing technology, there is a need to develop new equipment to reduce costs while expanding the range of processing to promote bonnet polishing technology to more polishing processes.

Wan et al. [20] proposed an effective method for reducing edge errors in the polishing of large mirrors. The form quality convergence rate can be improved by adjusting the amount of polishing removal. Liu et al. [21] combined CCOS technology and robot-assisted processing for the polishing of SiC mirrors. The final surface shape error of the primary mirror was 11.4 nm RMS, and the tertiary was 12.1 nm RMS. The capability of off-axis aspheric mirror fabrication on the robot polishing system was verified. Nagata et al. [22] successfully implemented a CAD/CAM-based position/force control method for robot polishing of curved molds, and Dieste et al. [23] used a spherical robot for automatic grinding and polishing of metal workpieces. Walker et al. [24, 25] demonstrated preliminary work in robot smoothing using fixed and loose abrasives, with the robots under direct and versatile control of an extended version of the Zeeko Tool Path Generator software suite.

In summary, robot-assisted polishing is receiving increasing attention, and achieving efficient and high-precision polishing is one of the research hotspots. In this study, a six-axis serial robot device and a bonnet polishing tool are used as the research objects. A robot feed polishing motion model was established for the polishing of large-diameter motion model, an optimal efficiency control algorithm was proposed, and polishing

experiments were conducted to verify the polishing capability of the robotic bonnet polishing system.

2 Modeling for Robotic Precession Movement

When polishing optical components with a bonnet tool, it is necessary to maintain the bonnet axis at a constant precession angle to the workpiece's normal. Therefore, the end-tool coordinate system of the robot must be controlled to maintain its corresponding poses. There are numerous ways to control the end-tool pose of a robot, and different companies use different control strategies for their robots. Robots manufactured by ABB are controlled by position coordinate values and quaternions. Therefore, in the robotic bonnet polishing system, the bonnet can consistently maintain the precession pose with the workpiece in the following two steps: (1) Determine the coordinates of the polishing point. The polishing path is discretized, the discrete target point coordinates are obtained, and the position coordinates of the airbag ball center (TCP) are obtained by coordinate transformation. (2) Determine the incoming pose. According to the transformation relationship of different coordinate systems, the transformation matrix and quaternions are obtained.

The precession model of robotic bonnet polishing is shown in Figure 1. The workpiece coordinate system $O_w X_w Y_w Z_w$, tool coordinate system $O_t X_t Y_t Z_t$ and local coordinate system $O_p X_p Y_p Z_p$ were established at the workpiece center, bonnet tool center, and arbitrary polishing point, respectively. The workpiece coordinate system direction was consistent with the robotic base coordinate system $O_o X_o Y_o Z_o$, and the tool coordinate system was in the same direction as the sixth joint coordinate system. In the local coordinate system, Z_p is opposite to the normal vector of the polishing point, Y_p is the tangent direction on the ZY section, and X_p direction is uniquely determined by the right-handed principle. Here, ρ denotes the precession angle and ε represents the angle between the spin axis of the bonnet in the $X_t Y_t$

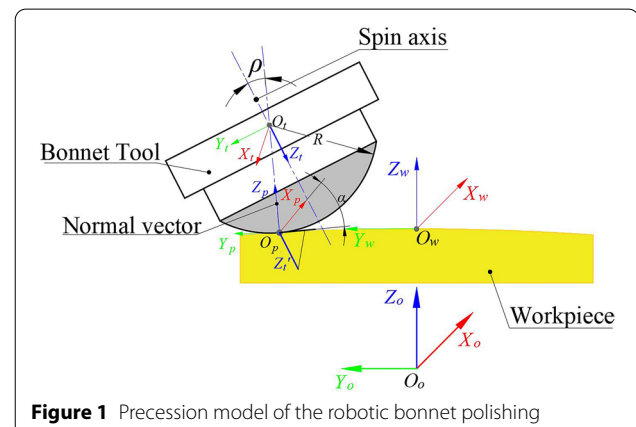


Figure 1 Precession model of the robotic bonnet polishing

and X_t directions. Based on the definition of the precession angle, ε is between 0° – 360° , and R represents the bonnet radius.

The surface function of the large axisymmetric aspheric optical component can be expressed as Eq. (1).

$$F(x y z) = 0. \quad (1)$$

Eq. (2) is a normal vector of polishing point $(x_p y_p z_p)$.

$$\mathbf{n}_z^p = \left[\frac{F'_x(x_p y_p z_p)}{c_1} \quad \frac{F'_y(x_p y_p z_p)}{c_1} \quad \frac{F'_z(x_p y_p z_p)}{c_1} \right]. \quad (2)$$

Tangent vector on ZY section of polishing point can be given as Eq. (3).

$$\mathbf{n}_y^p = \left[0 \quad \frac{y_p}{c_2} \quad \frac{-y_p F'_x / F'_z}{c_2} \right]. \quad (3)$$

Combined with Eqs. (2) and (3), the vector in X direction can be expressed as Eq. (4):

$$\mathbf{n}_x^p = \left[\frac{-(F'_z F'_x + F'_x F'_y) / F'_z}{c_1 c_2} \quad \frac{F'_x F'_x / F'_z}{c_1 c_2} \quad \frac{F'_x}{c_1 c_2} \right]. \quad (4)$$

where $c_1 = \sqrt{(F'_x)^2 + (F'_y)^2 + (F'_z)^2}$, $c_2 = \sqrt{y_0^2 + (-y_0 F'_x / F'_z)^2}$.

Subsequently, the transformation matrix wR_p of the local coordinate system $O_p X_p Y_p Z_p$ to the workpiece coordinate system $O_w X_w Y_w Z_w$ is obtained.

Since the angle ε can vary within the range of 0° to 360° , the spin axis of bonnet precession polishing are distributed on the conical plane as shown in Figure 2.

Based on the coordinate transformation, the transformation relation, the local coordinate system $O_p X_p Y_p Z_p$ to the tool coordinate system $O_t X_t Y_t Z_t$ can be expressed as Eq. (5).

$${}^pR_t = \text{Rot}(Z, \varepsilon) \text{Rot}(Y, \rho) \text{Rot}(Z, -\varepsilon). \quad (5)$$

Accordingly, the position of the bonnet center can be expressed as Eq. (6).

$$\begin{cases} x_t = x_p + (F'_x \times r) / c_1, \\ y_t = y_p + (F'_y \times r) / c_1, \\ z_t = z_p + (F'_z \times r) / c_1. \end{cases} \quad (6)$$

The pose transformation matrix as Eq. (7) can be obtained as follows:

$${}^wR_t = {}^wR_p {}^pR_t = [nx \ ny \ nz]. \quad (7)$$

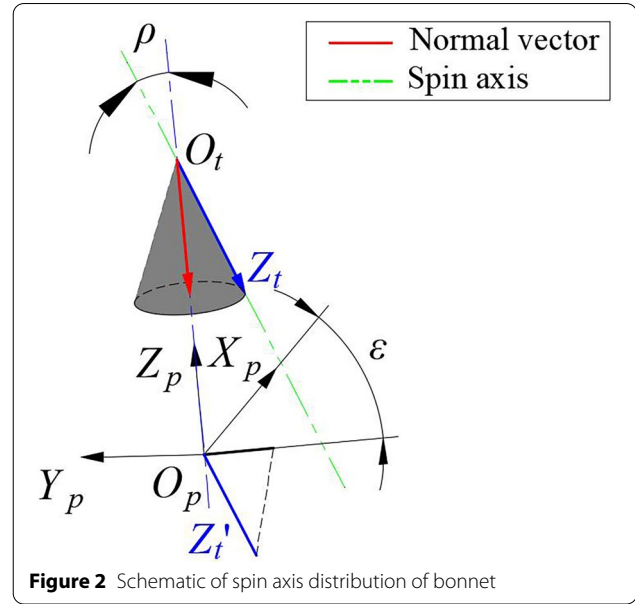


Figure 2 Schematic of spin axis distribution of bonnet

In the actual motion programming of the robot, the transformation matrix must be converted into quaternions $[q_1 \ q_2 \ q_3 \ q_4]$ according to certain rules, as shown in Eq. (8).

$$\begin{cases} q_1 = \frac{\sqrt{nx_1 + ny_2 + nz_3 + 1}}{2}, \\ q_2 = \frac{\sqrt{nx_1 - ny_2 - nz_3 + 1}}{2}, \text{sgn}(q_2) = \text{sgn}(ny_3 - nz_2), \\ q_3 = \frac{\sqrt{ny_2 - nx_1 - nz_3 + 1}}{2}, \text{sgn}(q_3) = \text{sgn}(nz_1 - nx_3), \\ q_4 = \frac{\sqrt{nz_3 - nx_1 - ny_2 + 1}}{2}; \text{sgn}(q_4) = \text{sgn}(nx_2 - ny_1). \end{cases} \quad (8)$$

where the sign of q_1 is always positive, and the values of the quaternions are determined by the surface function $F(x y z)$, precession-angle ρ , and angle ε . The position and pose quaternions of the end-effector can be obtained to control the robot's motion by establishing a movement model. Since the value of angle ε , which changes between 0° – 360° , can be determined using a feasible control algorithm, the pose of the bonnet tool can be determined accordingly.

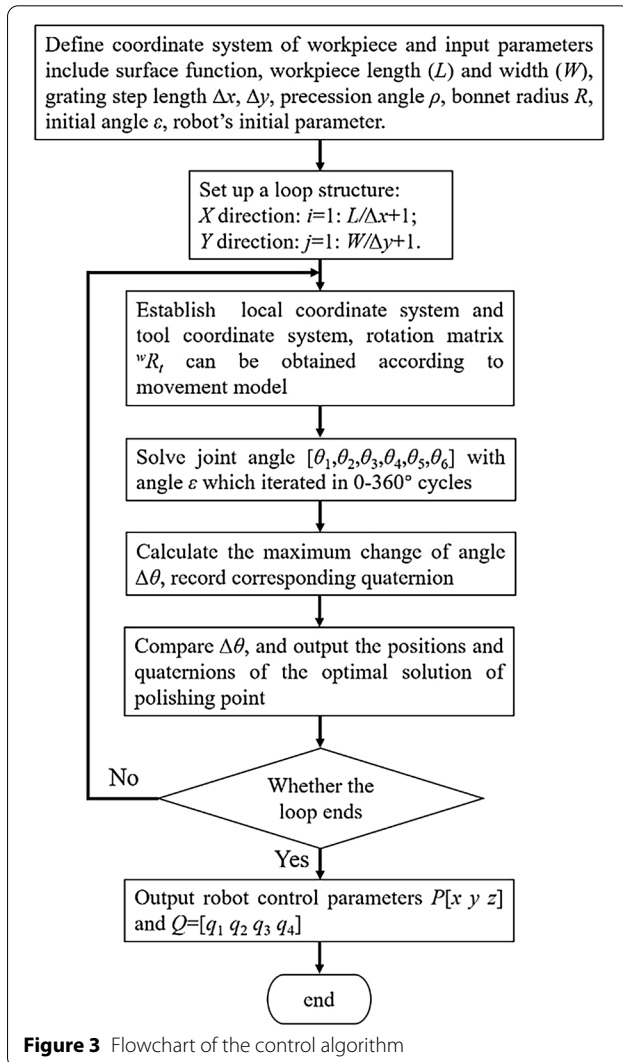
3 Control Algorithm for Robotic Bonnet Polishing Movement

Reducing the processing cycle and improving the processing efficiency in industrial production are beneficial for increasing profits. Optimizing the feeding time is an effective and feasible method to improve the polishing

efficiency. Six-axis industrial robots adopt a six-axis simultaneous-motion mode. For a given feeding rate, the feeding time depended on the time required for the maximum joint from point to point. Therefore, the maximum change in the angle of the robotic joint rotation at any two points was considered as the optimization target, as shown in Eq. (9).

$$\Delta\theta = \max[|\Delta\theta_1| |\Delta\theta_2| |\Delta\theta_3| |\Delta\theta_4| |\Delta\theta_5| |\Delta\theta_6|]. \quad (9)$$

The bonnet poses were optimized to minimize the change in the angle between any two polishing points during the polishing movement. The rotating angles of the six robotic joints were solved by combining the forward and inverse kinematics of the robot in MATLAB2016b using the transformation matrix of the coordinate system. The flow of the control algorithm is illustrated in Figure 3.



4 Simulation and Experiment

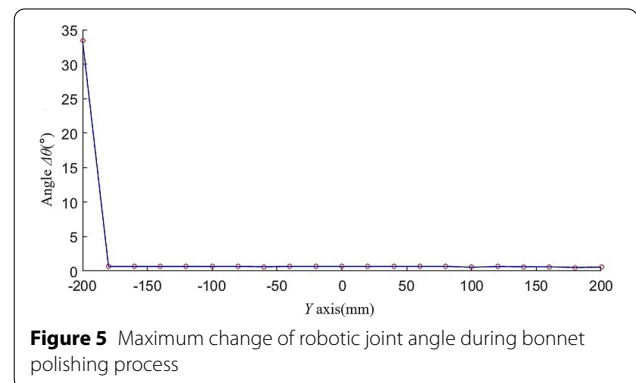
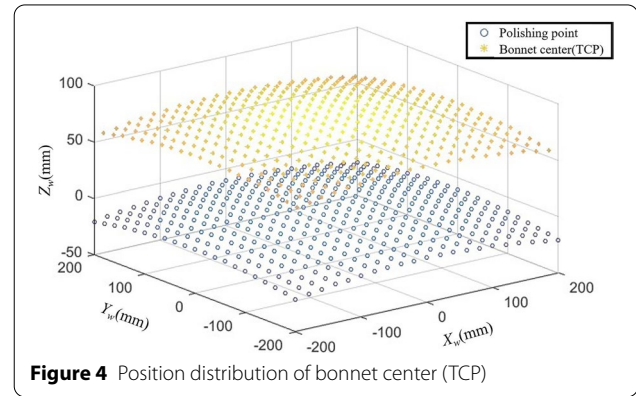
The surface function of the aspheric optical workpiece is shown as Eq. (10).

$$Z = \frac{Cx^2}{1 + \sqrt{1 - (1+k)C^2X^2}} - \sum_{i=1}^n (a_i x^i), \quad (10)$$

where C denotes the curvature of the aspheric base circle; k is the conicity of the aspheric surface, and a_i is the aspheric higher-order term coefficient.

The size of the polishing area was 400 mm × 400 mm, and the precession angle ρ was 20°. An XY-linear-grating polishing path was adopted, and the path spacing and polishing step length were 20 mm. A movement model and control strategy were used for the simulation. The position distribution of the bonnet center (TCP) during the bonnet polishing process is shown in Figure 4. The angle change value and program parameters of the robot were obtained via pose control. The curve of the maximum change in the robotic joint angle from the initial state of bonnet polishing to the first grating scanning path is shown in Figure 5.

The distribution of the bonnet center is consistent with that of the aspheric surface, which verifies the accuracy



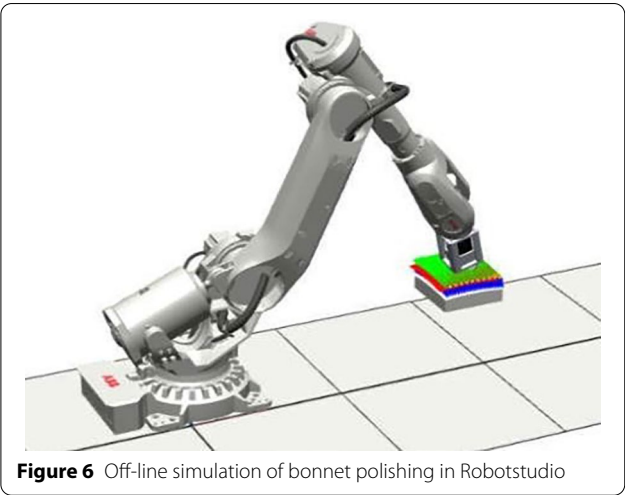


Figure 6 Off-line simulation of bonnet polishing in Robotstudio

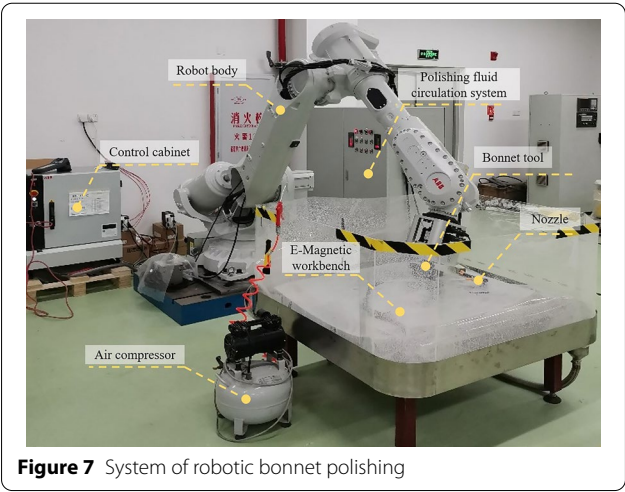


Figure 7 System of robotic bonnet polishing

of its position control. In pose control, a large angular travel is required to move from the initial position to the first polishing point, whereas the aspheric curvature changes slightly between any two polishing points, so that the robot’s joint angles changes slightly. The control code for the robot generated by the program was imported into Robotstudio, a special simulation software for ABB robots, to ensure the accuracy and effectiveness of the control program. Figure 6 presents an offline simulation of bonnet polishing in Robotstudio. The simulation results demonstrate that the control method is accurate and effective. The simulation time was 126.9 s at a speed rate of 100 mm/s, regardless of the polishing dwell time.

The control algorithm was used to polish the plane optical element using the robotic bonnet polishing system, as shown in Figure 7. The polishing area was 40 mm × 40 mm, and the velocity of TCP was 0.5 mm/s, additional polishing parameters are listed in Table 1.

Table 1 Area polishing parameters

Bonnet’s radius (mm)	Polishing area (mm)	Precession angle (°)	Z-offset (mm)	Inflation pressure (MPa)	Rotational speed (r/min)
80	40×40	20	0.4	0.2	750

Table 2 Information for the ABB-IRB6700 robot

Operating range (m)	Bearing capacity (kg)	Repetitive positioning accuracy (mm)	Repetitive path accuracy (mm)	Total mass (kg)
2.6	200	0.05	0.1	1170

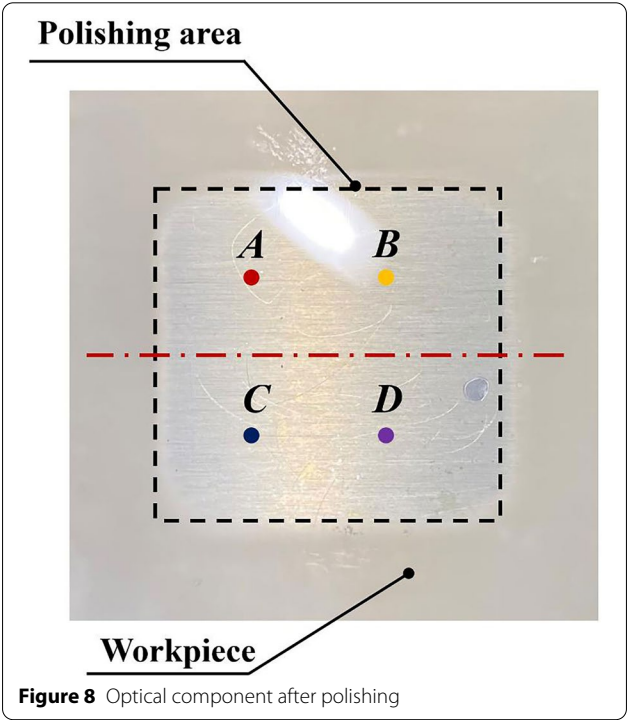
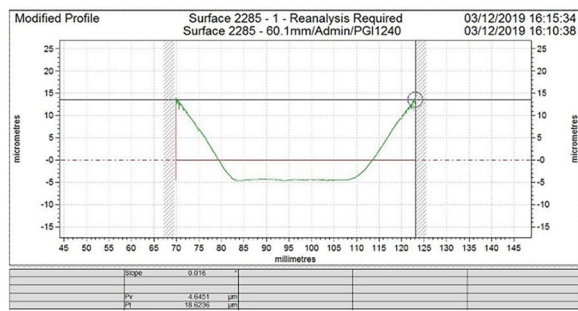


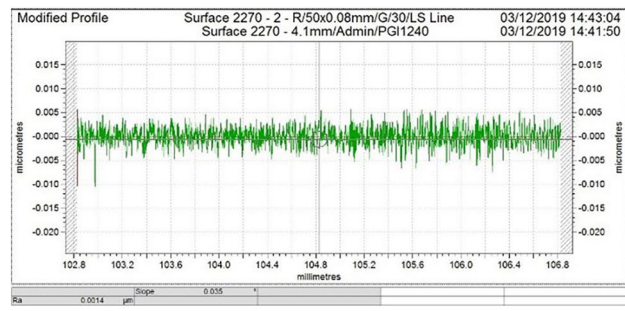
Figure 8 Optical component after polishing

The model of the industrial robot used in the experimental setup is ABB-IRB6700, and its information is listed in Table 2.

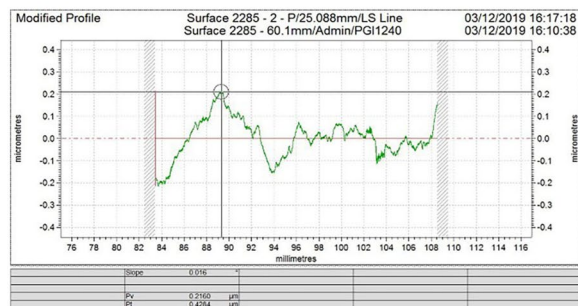
There was an obvious polishing area after polishing, as shown in Figure 8. A Taylor Hobson Form Talysurf was used to detect the polished area, and the removal depth was obtained by detecting the middle section of the polished area. The results are presented in Figure 9. Here, Figure 9(a) represents the surface profile along the red line, which is shown in Figure 8, and the removal depth



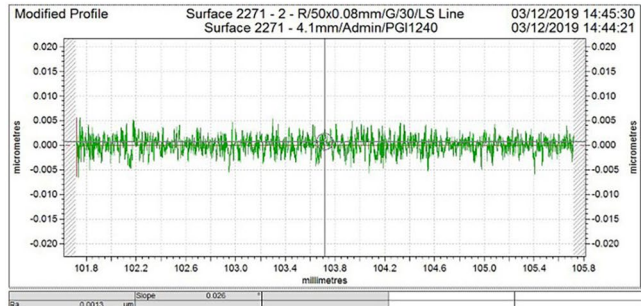
(a) Surface profile along the red line



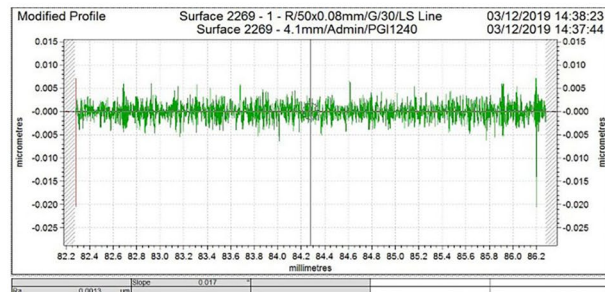
(d) Roughness measurement result at point B



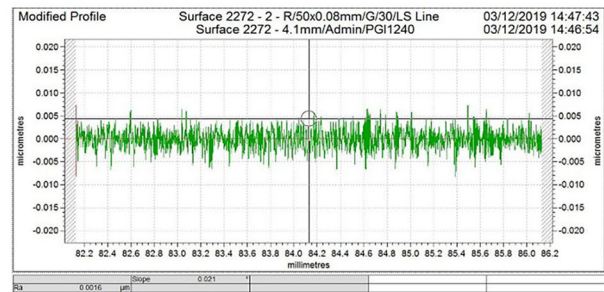
(b) Surface profile along part of the red line



(e) Roughness measurement result at point C



(c) Roughness measurement result at point A



(f) Roughness measurement result at point D

Figure 9 Measurement results by Taylor Hobson Form Talysurf

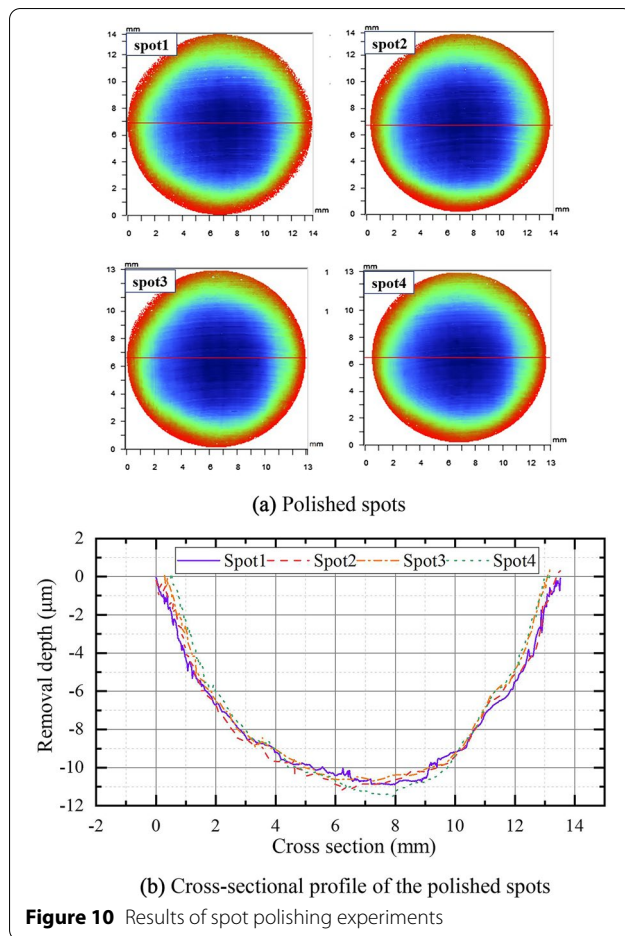
was measured at 18 μm ; and Figure 9(b) is the surface profile measured in part of the red line, with a PV value of 0.4 μm . Finally, the roughness at points A, B, C and D was shown in Figure 9(c), (d), (e), and (f), the average Ra value is 1.4 nm.

It is evident from the experimental results that the robotic bonnet polishing system can polish optical components to obtain low roughness, indicating that the technology can be applied to the precision polishing process of optical components. However, as a fast polishing technique, the material removal efficiency of this technique must also be considered. Four repetitions of the spot polishing experiments were carried out to obtain the material removal rate of the bonnet polishing system. The experimental parameters are listed in Table 3. There

Table 3 Spot polishing parameters

Bonnet's radius (mm)	Dwell time (s)	Precession angle ($^{\circ}$)	Z-offset (mm)	Inflation pressure (MPa)	Rotational speed (r/min)
80	80	20	0.6	0.2	500

are four main process parameters, which are precession angle, Z-offset, inflation pressure and rotational speed. The experimental results are shown in Figure 10(a). The removal depth was obtained by obtaining the data of the middle section of the four polished spots, as shown in Figure 10(b). The average removal depth was 11.08 μm , the material removal rate was 0.138 $\mu\text{m/s}$. The



experiments verified the accuracy of the control algorithm and the high efficiency of bonnet polishing.

5 Conclusions

- (1) In this study, the dynamic characteristics of bonnet polishing were analyzed, and a precession motion model of robotic bonnet polishing was proposed.
- (2) Inverse solutions of the robot motion angles were obtained using the robot toolbox in MATLAB2016b. Based on the special simulation software for ABB robots, the accuracy of the precession control algorithm of robot bonnet polishing for the aspheric component was verified.
- (3) The algorithm was successfully applied to the polishing experiment, and R_a was 1.4 nm when the polished surface sampling length was 4 mm. The material removal rate from the spot-polishing experiment was $0.138 \mu\text{m/s}$. Therefore, the robotic bonnet polishing system developed in this study proved to have good polishing ability.

Acknowledgements

Not applicable.

Author contributions

ZW was in charge of the whole trial. XH conducted experiments and data analysis. ZL wrote the manuscript. All authors read and approved the final manuscript.

Authors' Information

Xuepeng Huang, born in 1995, is currently a Ph.D. candidate at *Xiamen University, China*.

Zhenzhong Wang, born in 1981, is currently an associate professor at *Shenzhen Research Institute of Xiamen University, China*. He received his Ph.D. degree from *Xiamen University, China*. His research interests include intelligent manufacturing and precision engineering.

Zewen Lin, born in 1995. He received his master's degree from *Xiamen University, China*.

Funding

Supported by Science and Technology Projects of Shenzhen (Grant No. JCYJ20180306172924636).

Competing Interests

The authors declare no competing financial interests.

Author Details

¹Department of Mechanical and Electrical Engineering, Xiamen University, Xiamen 361005, China. ²Shenzhen Research Institute of Xiamen University, Shenzhen 518057, China.

Received: 10 November 2020 Revised: 19 May 2022 Accepted: 24 May 2022

Published online: 11 June 2022

References

- [1] David Walker, David Brooks, Richard Freeman, et al. First aspheric form and texture results from a production machine embodying the precession process. *Proceedings of SPIE*, 2001, 4451: 267-276.
- [2] David Walker, David Brooks, Andrew King, et al. The 'Precessions' tooling for polishing and figuring flat, spherical and aspheric surfaces. *Optics Express*, 2003, 11(8): 958-964.
- [3] David Walker, Richard Freeman, Gerry Mccavana, et al. Zeeko/UCL process for polishing large lenses and prisms. *Proceedings of SPIE*, 2002, 4411:106-111.
- [4] Guoyu Yu, David Walker, Hongyu Li. Research on fabrication of mirror segments for E-ELT. *Proceedings of SPIE*, 2012, 8416: 1-6.
- [5] Guoyu Yu, Walker David, Hongyu Li. Implementing a grolishing process in Zeeko IRP machines. *Applied Optics*, 2012, 51(27): 6637-6640.
- [6] Anthony Beaucamp, Yoshiharu Namba, Phillip Charlton, et al. Finishing of EUV photomask substrates by CNC precessed bonnet polisher. *Proceedings of SPIE*, 2013, 8880:1-6.
- [7] Bo Gao, Yingxue Yao, Dagang Xie, et al. Development and property test of bonnet polishing tool. *Modern Manufacturing Engineering*, 2004, (10): 52-54. (in Chinese)
- [8] Jianfeng Song, Yingxue Yao, Dagang Xie, et al. Study on ultra-precision bonnet tool polishing method. *Journal of Huazhong University of Science and Technology(Natural Science Edition)*, 2007, (S1): 104-107. (in Chinese)
- [9] Jincheng Gong, Dagang Xie, Jianfeng Song, et al. Study on influences of processing parameters on polishing spot for curved optical work-piece in bonnet polishing. *Journal of Yanshan University*, 2008, (3): 197-200. (in Chinese)
- [10] Bo Gao, Yingxue Yao, Dagang Xie, et al. Movement modeling and simulation of precession mechanisms for bonnet tool polishing. *Chinese Journal of Mechanical Engineering*, 2006(2): 101-104. (in Chinese)
- [11] Shunzhou Yu, Yingxue Yao. Study of post-processing algorithm for bonnet polishing CNC machine. *Machinery*, 2007(2): 16-18. (in Chinese)

- [12] Ri Pan, Wei Yang, Zhenzhong Wang, et al. Controlled bonnet polishing system for large aspheric lenses. *High Power Laser and Particle Beams*, 2012, 24(6): 1344-1348. (in Chinese)
- [13] Ri Pan, Zhenzhong Wang, Yinbiao Guo, et al. Movement modeling and control of precession mechanism for bonnet tool polishing large axisymmetrical aspheric lenses. *Journal of Mechanical Engineering*, 2012, 48(11): 183-190. (in Chinese)
- [14] Chunjin Wang, Yinbiao Guo, Zhenzhong Wang, et al. Dynamic removal function modeling of bonnet tool polishing on optics elements. *Journal of Mechanical Engineering*, 2013, 49(17): 19-25. (in Chinese)
- [15] Ri Pan, Zhenzhong Wang, Chunjin Wang, et al. Control techniques of bonnet polishing for free-form optical lenses with precession. *Journal of Mechanical Engineering*, 2013, 49(03): 186-193. (in Chinese)
- [16] Chenchun Shi, Yunfeng Peng, Liang Hou, et al. Improved analysis model for material removal mechanisms of bonnet polishing incorporating the pad wear effect. *Appl. Opt.*, 2018, 57(25): 7172-7186.
- [17] Chenchun Shi, Yunfeng Peng, Liang Hou, et al. Micro-analysis model for material removal mechanisms of bonnet polishing. *Appl. Opt.*, 2018, 57(11): 2861-2872.
- [18] Zhongchen Cao, Chi Fai Cheung, Xing Zhao. A theoretical and experimental investigation of material removal characteristics and surface generation in bonnet polishing. *Wear*, 2016, 360-361:137-146.
- [19] Zhongchen Cao, Chi Fai Cheung. Multi-scale modeling and simulation of material removal characteristics in computer-controlled bonnet polishing. *International Journal of Mechanical Sciences*, 2016, 106:147-156.
- [20] Songlin Wan, Xiangchao Zhang, Wei Wang, et al. Edge control in precision robotic polishing based on space-variant deconvolution. *Precision Engineering*, 2019, 55: 110-118.
- [21] Haitao Liu, Fengtao Yan, Wenchuan Zhao, et al. Fabrication of SiC off-axis aspheric mirror by using robot polishing. *The European Physical Journal Conferences*, 2019, 215: 9004.
- [22] Fusaomi Nagata, Tetsuo Hase, Zenku Haga, et al. CAD/CAM-based position/force controller for a mold polishing robot. *Mechatronics*, 2007, 17(4-5): 207-216.
- [23] J. A. Dieste, A. Fe Rnández, D. Roba, et al. Automatic grinding and polishing using spherical robot. *Procedia Engineering*, 2013, 63: 938-946.
- [24] David Walker, Christina Dunn, Guoyu Yu, et al. The role of robotics in computer controlled polishing of large and small optics. *Proceedings of SPIE*, 2015, 9575: 1-9.
- [25] David Walker, Guoyu Yu, Caroline Gray, et al. Process automation in computer controlled polishing. *Advanced Materials Research*, 2016, 1136: 684-689.

Submit your manuscript to a SpringerOpen[®] journal and benefit from:

- Convenient online submission
- Rigorous peer review
- Open access: articles freely available online
- High visibility within the field
- Retaining the copyright to your article

Submit your next manuscript at ► [springeropen.com](https://www.springeropen.com)